



An improved fuzzy logic control-based MPPT method to enhance the performance of PEM fuel cell system

Mokhtar Aly¹ · Hegazy Rezk^{2,3}

Received: 28 November 2020 / Accepted: 4 October 2021 / Published online: 22 October 2021
© The Author(s), under exclusive licence to Springer-Verlag London Ltd., part of Springer Nature 2021

Abstract

Recently, wide installations of photovoltaic (PV) systems have been achieved in the electrical power systems. However, fluctuated output power of the PV generation and/or fluctuated load demands represent critical factors for the operation of PV systems. Thence, energy storage systems (ESSs) are highly needed for improving the supply reliability of PV generation systems. Among existing ESSs, the proton exchange membrane fuel cell (PEMFC) systems represent long-lifetime, efficient, and cost-effective solutions for PV systems. However, nonlinear behaviour exists in the output of PEMFC systems, which depends on the operating cell temperature, and the membrane water contents. The output of PEMFC has a unique operating maximum power point (MPP) for each operating combination of membrane water content and temperature, which requires MPP tracking (MPPT) control loop. Therefore, this paper presents a fuzzy logic control (FLC) MPPT method for enhancing the operation of PEMFC systems. The traditional MPPT methods in the literature employ three sensors, including voltage, water content, and temperature. The proposed controller employs only the PEMFC output current and voltage electrical signals. Compared to the classical fixed step size perturb and observe (P and O) and hill climbing MPPT methods, the proposed method represents variable step size MPPT method. In addition, compared to the widely employed incremental conductance (INC) and incremental resistance (INR) MPPT methods, the proposed method benefits the wide operating and adaptive step size MPPT operation due to using the FLC approach. The proposed method is simple and can be implemented using low cost microcontrollers. The design procedures, operating principle, and performance verification of the proposed method are presented in this paper.

Keywords Fuzzy logic control · MPPT · Proton exchange membrane

1 Introduction

In recent decades, using traditional fossil fuels in electrical power generation has faced wide reduction due to their negative impacts on the environment and their limited existence. The renewable energy-based clean generation systems have shown effective alternative solutions for the replacement of fossil fuels [1–4]. However, the new

renewable sources are continually fluctuating in nature, which reduces their effectiveness [5]. In addition, the existing electrical loads in the utility grids are also continuously fluctuating. Thence, several applications of energy storage systems (ESSs) have been presented for grid-tied renewable clean energy sources [6]. During the day-time, the extra power from the photovoltaic (PV) source is stored in the ESSs to be used during the night time [7].

There are several existing ESS technologies in the literature, which are different in their operating mechanisms, operating performance, and their cyclic efficiencies. The widely used battery ESSs suffer from short lifecycle operating time, low cyclic efficiency, and high maintenance cost [6, 8]. Among the available ESSs, the fuel cell (FC) ESSs represent low noise, low cost, efficient, and environmentally friendly ESSs. The extra available power

✉ Hegazy Rezk
hr.hussien@psau.edu.sa

¹ Facultad de Ingeniería y Tecnología, Universidad San Sebastián, Bellavista 7, Santiago, Chile

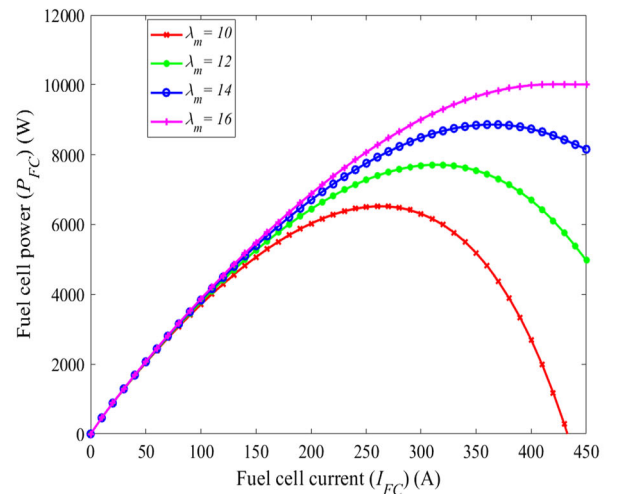
² College of Engineering at Wadi Addawaser, Prince Sattam Bin Abdulaziz University, Al-Kharj 11911, Saudi Arabia

³ Electrical Engineering Department, Faculty of Engineering, Minia University, Minia 61517, Egypt

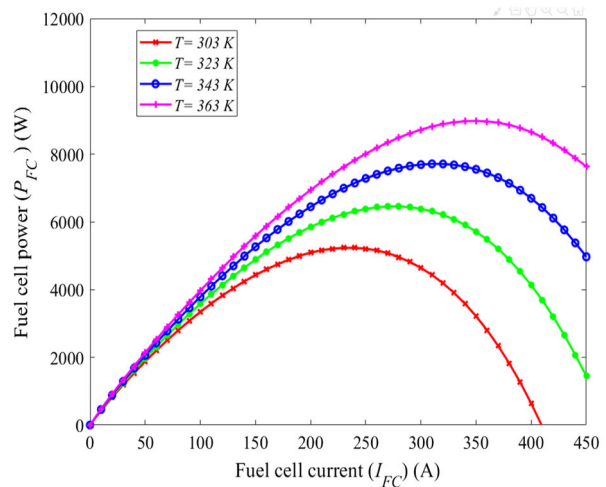
from the PV source are utilized to generate hydrogen by the electrolyzer [9, 10]. Afterwards, the generated hydrogen is stored and employed as powering source for the FC. The proton exchange membrane FC (PEMFC) type represents the most-widely utilized FC due to its lighter weight, faster start-up, lower operating temperature, and higher power density. Therefore, wide applications of PEMFCs have been found in electrical vehicles, renewable energy applications, etc. [11, 12].

PEMFCs have found wide range of applications with wide operating range of output power [13–15]. Several evaluation methods have been presented in the literature based on economic analysis [16], and experimental analysis [17]. In [18], PEMFCs have been utilized for the distributed power generation systems. The main key factors behind this application are their high operating efficiency, high power density, and reduced environmental impacts. Additionally, the application of hybrid PEMFC system for the MWE-scale clean power generation systems has been investigated in [19]. In which, PEMFCs have proven economic and technical feasibility for large-scale power applications. In [20], PEMFCs have been applied for residential applications. In [21], joint utilization of PEMFC with the combined heat and power (CHP) has been presented for residential buildings to meet the thermal and electrical loading demands. The PEMFC systems have been also presented for unmanned aerial vehicle (UAV) applications [22, 23]. Moreover, PEMFCs have found wide employment in electric vehicle applications [24, 25]. Furthermore, extensive applications of PEMFCs for hybrid tramway transportation systems have been investigated in the literature [26, 27].

However, the operating characteristics of PEMFC have nonlinear behaviour in its output waveforms. The main influencing factors are the membrane water content and the temperature. Figure 1 shows the output of the implemented PEMFC model for the PEMFC power (P_{FC})—PEMFC current (I_{FC}) relation at different membrane water content (λ_m), and at different temperature (T). The waveforms are based on the detailed model of PEMFCs that was provided in [28]. It can be seen that the output is highly dependent on the operating conditions of λ_m and T . It can be seen also that the operating curve has unique operating maximum power point (MPP), and hence there are a high need for MPP tracking (MPPT) controller for efficient operation of PEMFCs. Determining the MPP operating point would maximize the utilized electrical energy from the PEMFC. Several studies have been presented in the literature for comparing the operation of PEMFCs with/without MPPT control. The control of MPPT is achieved through determine the optimum duty cycle for the boost dc/dc converter, which interfaces and steps up the output voltage of the PEMFC.



(a) The Power-Current Curves at different (λ_m)



(b) The Power-Current Curves at different temperature (T)

Fig. 1 The nonlinear behaviour of PEMFC ESSs

There are wide-existing MPPT techniques in the literature. The traditional hill climbing (HC), and perturb and observe (P and O) methods have been widely applied in the literature [29]. In addition, the P and O MPPT has been utilized with the interleaved boost dc/dc converters for electric vehicle (EV) applications [29]. The P and O is capable of operating the PEMFC at its MPP at different operating conditions. However, they operate with fixed step size (FSS), and their performance is sensitive to the selected step size.

From another side, the variable step size (VSS) MPPT methods have shown better alternatives to the fixed step size MPPT solutions. In [30], incremental conductance (INC) has been applied to PEMFC systems. The incremental resistance (INR) has been proposed in [31] for improving the performance of PEMFCs. In [32], proportional-integral-derivative (PID) tuned with the grey wolf optimization (GWO) and the dP/dI control has been

presented. This method can achieve fast tracking of the MPP at different operating scenarios. Another nonlinear PID controller has been presented and tuned with the teaching learning-based optimizer (TLBO) method [33]. Another golden section search (GSS) MPPT controller has been presented in [34]. The presented method is advantageous at achieving variable step size MPPT control of PEMFC systems.

The interleaved two-phase boost power conversion has been utilized with the chaotic modified whale optimization algorithm to maximize the output power of PEMFCs [35]. Another solution has been proposed through using artificial neural network precise modelling of PEMFCs [36]. The adaptive neuro-fuzzy inference system (ANFIS) has been also employed for MPPT control in [37]. The ANFIS-based MPPT method has proven superior performance compared to the other existing MPPT techniques. Radial basis function network (RBFN) algorithm has been proposed in [38] for improving output power extraction of PEMFCs. However, this method requires extensive training data and complex modelling.

Additionally, the particle swarm optimization (PSO) and the PID controller have been presented for PEMFCs [39]. Another method based on neural network INC MPPT method for PEMFCs has been presented in [40]. The particle swarm optimization (PSO) and other optimization techniques were proposed as MPPT solutions for PEMFCs [39]. Moreover, the neural network-based MPPT solutions have been presented in the literature [40, 41]. The fuzzy logic control (FLC) has also found wide applications in MPPT in several applications [42–44]. The FLC systems have been utilized for various MPPT control [45], energy management [46], grid support [47], EVs applications [48], etc. In [28], the differential evolution optimization algorithm (DEOA) method has been presented for optimizing the performance of FLC MPPT for PEMFC applications. A reduced sensor MPPT method has been presented in [49] with using only the current sensor. Another hybrid P and O and type-2 FLC-based adaptive variable step size MPPT controller has been proposed in [50]. The presented algorithm can effectively optimize the design of FLC MPPT method. However, most of the existing PEMFC MPPT solutions utilize highly complex algorithms, costly sensors, deteriorated performance, and/or slow response.

Stimulated by the abovementioned issues of existing MPPT methods, this paper presents an improved fuzzy logic control (FLC) MPPT method for PEMFCs. The proposed design benefits the fast tracking, simple implementation, and the reduced sensors count and cost. The main contribution of this work can be highlighted as follows:

- Application and design method for the asymmetrical FLC-based MPPT method for efficient tracking of the maximum power of PEMFCs. The various designs of the FLC MPPT methods are introduced and compared to the proposed method.
- The proposed method represents an effective approach for reducing the steady state oscillations through the continuous tracking for the MPPT at different operating membrane water content and temperature operations. This in turn can lead to enhancing the operating lifetime of PEMFCs.
- The proposed FLC MPPT method is advantageous at fast tracking of the operating MPP without overshoot/undershoot spikes and with reduced settling times compared to the existing MPPT methods. A programmed FLC algorithm is implemented in Matlab to prove the superior performance of the proposed method compared to the other FLC design methods.

The remaining of the paper is organized as following: Sect. 2 presents the operating principles and design of the proposed FLC MPPT method. The simulation results of the proposed method are detailed in Sect. 3. Finally, the paper is concluded in Sect. 4.

2 The proposed FLC MPPT method

2.1 Modelling of PEMFC

The operation of PEMFC is dependent on the various operating conditions, including the membrane water content and temperature. The PEMFC output voltage is modelled with considering the activation, ohmic, and concentration loss terms. The output voltage of PEMFC can be modelled as follows [51]:

$$V_{FC} = E_{Nernest} - V_{act} - V_{ohm} - V_{con} \quad (1)$$

where V_{act} , V_{ohm} and V_{con} represent the activation, ohmic, and concentration loss terms, respectively. $E_{Nernest}$ represents reversible voltage at open FC terminals, which it is estimated as follows [52]:

$$E_{Nernest} = 1.229 - 8.5 \times 10^{-4}(T - 298.15) + 4.385 \times 10^{-5}T \ln(P_{H_2} + 0.5 \ln P_{O_2}) \quad (2)$$

whereas activation loss term can be estimated as following:

$$V_{act} = -[\xi_1 + \xi_2 T + \xi_3 T \ln(C_{O_2}) + \xi_4 T \ln(I_{FC})] \quad (3)$$

where ξ_1 , ξ_2 , ξ_3 , ξ_4 represent model coefficients and they are determined by experimental tests [52], and C_{O_2} represents the oxygen concentration in mol/cm³, which is calculated as following:

$$C_{O_2} = \frac{P_{O_2}}{5.08 \times 10^6 \times e^{\left(\frac{-498}{T}\right)}} \tag{4}$$

The value of ohmic loss term is resulting from ohmic resistance (R_M), and it is estimated as following:

$$V_{ohm} = I_{FC}R_M \tag{5}$$

whereas PEMFC ohmic resistance is determined as following [28]:

$$R_M = \frac{\rho_M l_M}{A} \tag{6}$$

where ρ_M represents resistivity of the membrane in Ω cm, l_M denotes to membrane thickness in cm, and A represents the FC active area in cm^2 . The resistivity of membrane is related to membrane water content in addition to the temperature as following [28]:

$$\rho_M = \frac{181.6 \left[1 + 0.03 \left(\frac{l_{FC}}{A} \right) + 0.0062 \left(\frac{T}{303} \right) \left(\frac{l_{FC}}{A} \right)^{2.5} \right]}{\left[\lambda_m - 0.634 - 3 \left(\frac{l_{FC}}{A} \right) \right] \exp \left[4.18 \left(\frac{T-303}{T} \right) \right]} \tag{7}$$

where λ_m represents operating membrane water content. The concentration loss term is related to hydrogen and oxygen transportation as follows:

$$V_{con} = \frac{-RT}{nF} \ln \left(1 - \frac{I_{FC}}{AI_{max}} \right) \tag{8}$$

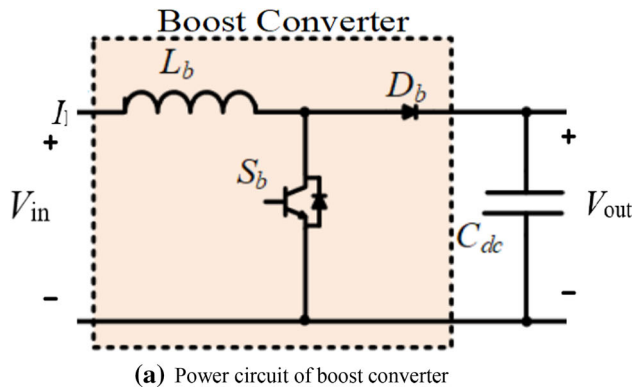
where n denotes to number of electrons that are included in reaction, and I_{max} represents current density limiting value in Acm^{-2} . The model parameters in [28] is used for the PEMFC model in this paper.

2.2 Operation of the boost dc/dc converter

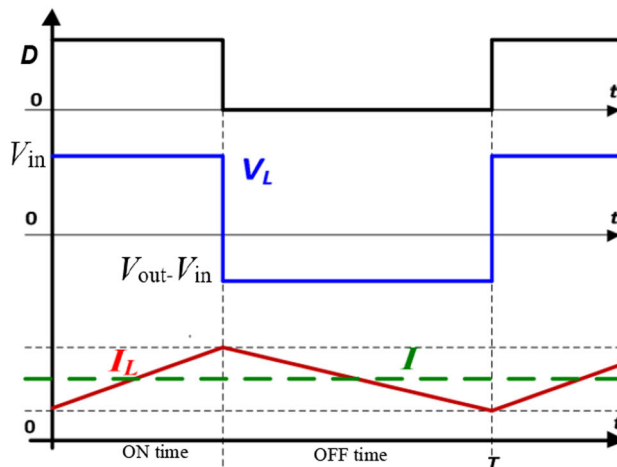
The power circuit of the PEMFC-based boost converter is shown in Fig. 2a. The output voltage of the PEMFC is utilized as input voltage for the boost converter, whereas the output voltage is fed to the battery ESS. The boost converter is driven through the duty cycle D , which is optimally determined according the MPPT algorithm [53]. The output of the MPPT controller is compared to a fixed frequency sawtooth generator to generate the gating pulse [54]. Hence, the output power of the PEMFC is maximized through the control of the boost converter duty cycle. The boost converter output voltage V_{out} is related to the input voltage V_{in} as following [53]:

$$V_{out} = \frac{1}{1-D} \times V_{in} \tag{9}$$

Figure 2b shows the operating waveforms of the boost dc/dc converter. During the duty cycle on period D , the input voltage is applied to the inductor of the boost. During this period, the inductor is charged and the slope of the change of inductor current is positive. Whereas, the voltage



(a) Power circuit of boost converter



(b) The operating waveforms of the boost converter

Fig. 2 The boost converter and its operating waveforms

($V_{out}-V_{in}$) is applied to the inductor during the OFF period of the duty cycle. During this period, the boost inductor is discharged and the change of inductor current is negative in this period. Due to the limitations of boost converter operation, the duty cycle operating range is limited within 0.1 to 0.9 range.

2.3 The proposed FLC MPPT method

The FLC method has found wide utilization in various applications due to its simplicity, independency on complex mathematical models, dealing with nonlinearities of systems. PEMFCs have shown nonlinear properties and their output is dependent on the membrane water content and the temperature. Hence, the FLC system is employed in this paper for achieving the MPPT control of PEMFCs. The proposed FLC method is based only on the measured electrical signals, including the PEMFC output voltage and current measurements. Therefore, it required lower number of sensors with dealing the nonlinear property of the PEMFC.

In this section, the operating principle and design for the proposed FLC MPPT method for PEMFC are introduced. Figure 3 shows the power circuit of the PEMFC system. The output of the cell is connected to boost dc-dc power converter for stepping-up the low output voltage of the cell in addition to performing the MPPT control. The sensed PEMFC voltage (V_{FC}) and current (I_{FC}) are sensed and used by the MPPT controller to drive the power switches with proper output duty-cycle.

The operating principle of the proposed FLC method has three main stages, which include the fuzzification, the fuzzy rule evaluation, and defuzzification stage. During fuzzification step, the input variables are used to determine the membership functions (MFs) of the input side of the FLC. The assigned MFs for input variables convert the measured signals into suitable fuzzy inputs. Then, the output of the fuzzification stage is evaluated according to the fuzzy rule set. In this stage, the controller action is defined according to the linguistic fuzzy rules. Finally, the output of the fuzzy rule evaluation stage is utilized as fuzzy output variable for each type from the actions of fuzzy input MFs. During the defuzzification step, the predicted value of output MFs are determined and then outputted to the PWM generator. The outputted change of the duty cycle ΔD by the FLC method is responsible for achieving the MPPT control. It can be estimated as following [55, 56]:

$$\Delta D = \frac{\sum_{i=1}^{49} W_i C_i}{\sum_{i=1}^{49} W_i} \tag{10}$$

where W_i represents the minimum number of MFs of the i th rule. Whereas, C_i denotes to the centre value for the output MF.

Figure 4 shows the main structure of the proposed FLC MPPT method. The signal conditional system generates the error E and the change of the error ΔE signals, which represent the inputs for the FLC system. The MPPT operation is related to the error signal as following:

$$E(k) = \frac{P_{FC}(k) - P_{FC}(k - 1)}{V_{FC}(k) - V_{FC}(k - 1)} \tag{11}$$

whereas the second input variable of the FLC method is calculated as following:

$$\Delta E(k) = E(k) - E(k - 1) \tag{12}$$

where $P_{FC}(k)$, and $P_{FC}(k - 1)$ are the measured PEMFC power at the sample instant k and $(k-1)$, respectively. Whereas, $V_{FC}(k)$, and $V_{FC}(k - 1)$ are the (k) th and $(k - 1)$ th measured PEMFC voltage, and the error signals $E(k)$, and $E(k - 1)$ are their corresponding error signals.

In the designed FLC MPPT method, the triangular shaped MFs are employed for representing the input and output variables. The triangular shaped MFs are represented by three points, i.e. $\tilde{M} = (l, m, u)$, where l , m , and u with $(l \leq m \leq u)$ represent the smallest, modal, and largest values in representing the triangular MF, respectively. The selected triangular shaped MF represents a continuous function within the interval $[0,1]$. The MF $\mu(x|\tilde{M})$ can be modelled as follows [57]:

$$\mu(x|\tilde{M}) = \begin{cases} (x - l)/(m - l), & l \leq x \leq m \\ (u - x)/(u - m), & m \leq x \leq u \\ 0, & \text{Otherwise} \end{cases} \tag{13}$$

The proposed method has two different input variables (E and ΔE), which includes seven fuzzy levels in their membership functions. They have three positive subsets, three negative subsets, and zero level subset. The output variable is represented by the change of the duty cycle

Fig. 3 The power and control system for PEMFC systems

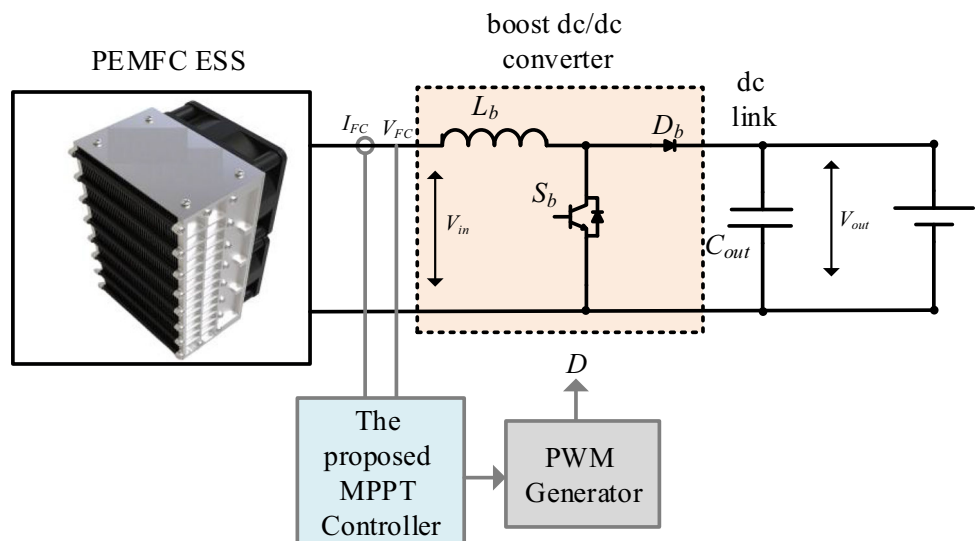
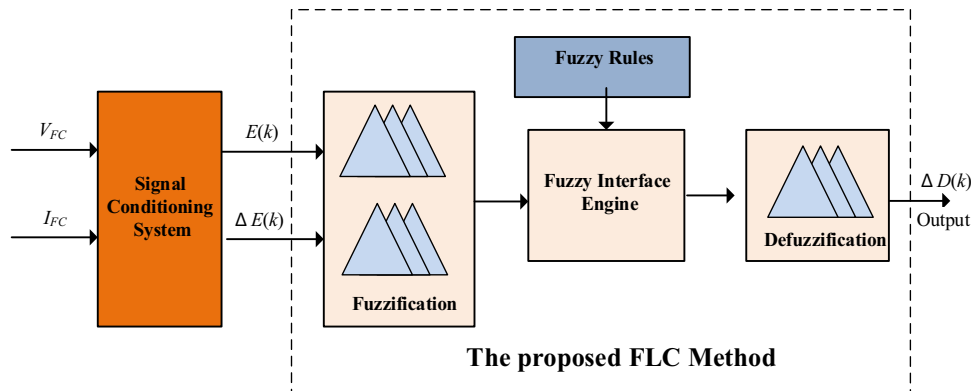


Fig. 4 The structure of the proposed FLC MPPT method



(ΔD), which is also divided into seven different subsets. Therefore, 49 total fuzzy rules exist in the implementation of the proposed method. After the estimation of (E and ΔE) input variables, the proposed FLC converts them into the corresponding linguistic variables. Afterwards, the proposed method generates the proper (ΔD) command as an output control signal. Table 1 shows the different fuzzy rules in the proposed method between the two input variables and the output variable. The triangular type of membership function is utilized for implementing the proposed FLC method due to its simplified implementation with low cost microcontrollers.

Figure 5 shows the power curves of PEMFCs at different operating temperature with adding the slope of $\Delta P_{FC}/\Delta V_{FC}$ to identify the location of MPPT. It can be seen that $\Delta P_{FC}/\Delta V_{FC}$ can be positive, negative, or zero value. The MPPT can be achieved when the PEMFC is operated at zero value of $\Delta P_{FC}/\Delta V_{FC}$, which represents the first input of the error signal E for the FLC MPPT method. Therefore, the MPPT algorithm has to continuously track the curve of $\Delta P_{FC}/\Delta V_{FC}$ to preserve the MPPT operating point. Whereas, the change in the error ΔE defines whether the PEMFC operating point is moving along the direction of MPPT. The tracking can be achieved through adjusting the change of the duty cycle output ΔD of the FLC method. In

the designed FLC MPPT methods, the ranges of input and output MFs are represented by three positive levels, three negative levels, and zero level. The fuzzy rules are extracted from the aforementioned analysis of the $\Delta P_{FC}/\Delta V_{FC}$ curves and their relation with the duty cycle of the converter. It can be seen from Table 1 that the fuzzy rules define the level of the outputted ΔD by the FLC MPPT method according to the level range of (E and ΔE) inputs of the FLC.

Figure 6 shows the various considered shapes of membership function of both the input and output variables of the proposed FLC MPPT method. The symmetrical are employed in the first and second designs with different gains of the (E and ΔE) input variables as shown in Fig. 6a, b, respectively. The symmetrical types of the FLC MPPT methods will be denoted as the (FLC 1) and (FLC 2) MPPT methods. Whereas, the third design is based on the asymmetrical shape of both the input and output membership functions. This design is considered as the proposed design of the FLC method and its performance would be compared to the other traditional MPPT methods and the other FLC designs. The asymmetrical design will be denoted by the (FLC 3) name in the results part. The FLC MPPT methods have been programmed in Matlab m-file so as to provide flexible platform for investigating the various designs for the FLC. The programmed FLC MPPT method provides more freedom in designing the input and output MFs.

Table 1 The different rules relating input and output variables in the proposed MPPT method

Input MFs	ΔE						
	N_3	N_2	N_1	Z_0	P_1	P_2	P_3
N_3	N_3	N_3	N_3	N_3	N_2	N_1	Z_0
N_2	N_3	N_3	N_3	N_2	N_1	Z_0	P_1
N_1	N_3	N_3	N_2	N_1	Z_0	P_1	P_2
E	Z_0	N_3	N_2	N_1	Z_0	P_1	P_2
	P_1	N_2	N_1	Z_0	P_1	P_2	P_3
	P_2	N_1	Z_0	P_1	P_2	P_3	P_3
	P_3	Z_0	P_1	P_2	P_3	P_3	P_3

3 Results and discussion

The PEMFC is modelled in Matlab with the boost dc-dc converter. In addition, the INC method is also implemented for performance comparison with the proposed method. The INC MPPT method is selected for the comparison in this paper due to its wide applications in the literature. Figure 7 shows the obtained results for the proposed algorithm in comparison to the widely used INC MPPT

Fig. 5 The operation of MPPT for the derivation of the fuzzy rules

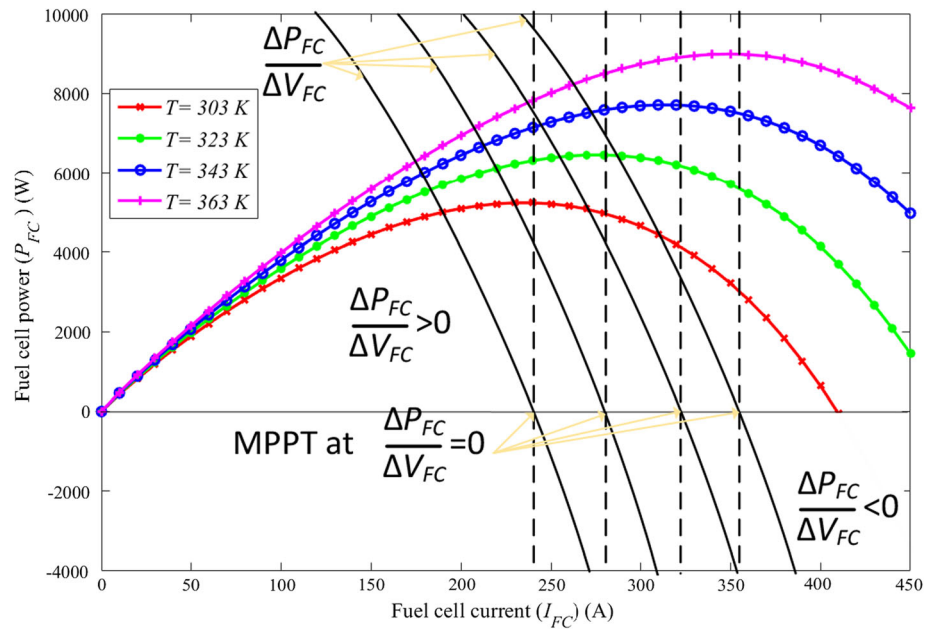
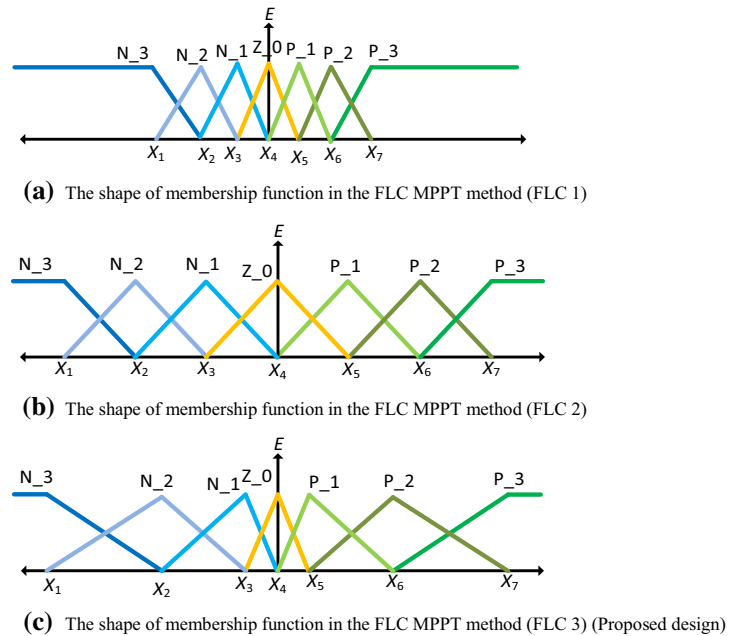


Fig. 6 The various membership function shapes in the proposed FLC MPPT method



method. Figure 7a shows the performance of the output power of the PEMFC at the normal starting operation. It can be seen that the proposed FLC method has fast steady state response with small output power overshoot/undershoot. The PEMFC reaches steady state in 0.01 s, compared to the 0.02 s for the INC MPPT method. Moreover, the INC has large fluctuations in the outputted power. It can be seen that performance of FLC MPPT methods is highly dependent on the design and selection of the MFs. The traditional FLC 2 method has slower response than the classical INC method and the proposed FLC method. This is a direct result of the designed limits and shape of the

input and output MFs in the FLC 2 method. The proposed FLC MPPT method is also adaptive at achieving fast transient response with good steady state performance.

Figure 7b shows the performance of the outputted PEMFC voltage for the proposed FLC method and the INC method. It is clear the large output voltage undershoot of the INC MPPT method. Whereas, the proposed FLC MPPT method has small undershoot of the outputted voltage from the PEMFC. The output current from the PEMFC for both MPPT algorithms is compared in Fig. 7c. The proposed FLC MPPT method has better output current response compared to the INC method, which has large output

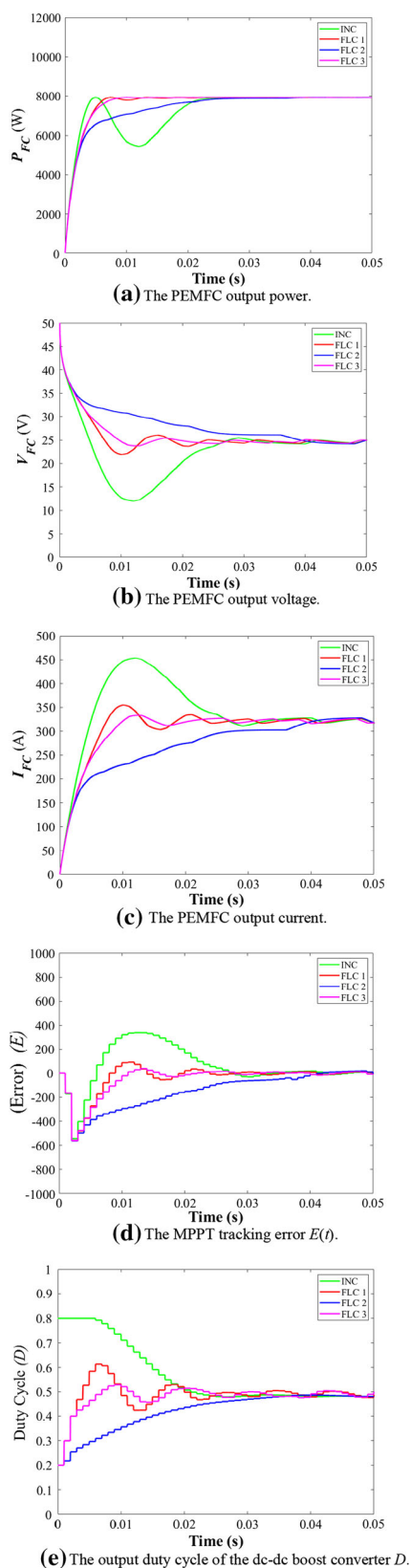


Fig. 7 Performance verification and comparison of the proposed FLC method at the transient starting

current overshoot. The large fluctuations of the INC can result in shortening the operating lifetime of the PEMFC and its interconnected power components.

The performance of the MPPT tracking methods can be evaluated with the rate of change of the output power with the voltage of the PEMFC. This term can be expressed by the error signal, which represents the first input for the FLC method. Figure 7d shows the performance comparison of the proposed FLC MPPT method with the INC MPPT method. The proposed FLC MPPT method has lower error signal, which reflects the faster MPPT tracking in the proposed method compared to the slower tracking of the INC method. The duty cycle comparison between the proposed algorithm and the other methods is shown in Fig. 7e. It can be seen that the proposed method can adjust the starting duty cycle with fast response.

Additionally, the proposed method is tested at the various step changes in the membrane water content. Figure 8a shows the tested scenario of membrane water content values. Figure 8b shows the response of the output power of the PEMFC for the different MPPT methods. The proposed method can achieve fast tracking of the MPPT of PEMFC. In addition, low fluctuations in the output power is obtained using the proposed method. The proposed method achieves reduced overshoot/undershoot in the outputted power of PEMFC. It has become clear that the proposed algorithm provides an efficient and stable MPPT control method for the different tested membrane water content scenarios.

Figure 8c shows the response of the PEMFC output voltage for the different compared MPPT methods. It can be seen that the proposed method maintain reduced overshoots/undershoots in the PEMFC output voltage. The proper design of the proposed FLC method results in the reduction of the PEMFC voltage fluctuation at the various changes in the membrane water content. Additionally, the output current of the PEMFC under the various MPPT methods is shown in Fig. 8d. A high reduction of the PEMFC output current is obtained using the proposed method. Therefore, the proposed method can achieve prolonged lifetime of the PEMFC due to the reduction of the PEMFC output voltage and current fluctuations.

From another side, the proposed method is compared to the other existing methods at step changes in the temperature. Figure 9a shows the temperature waveforms for the tested scenarios. Figure 9b shows the response of the PEMFC output power under the different studied MPPT methods. The proposed method provides smooth output power at the different studied scenarios. In addition, low fluctuations are obtained at the various temperature steps under the proposed method. This in turn results at providing smooth power management of the PEMFC at the various applications with different steps. Moreover, the

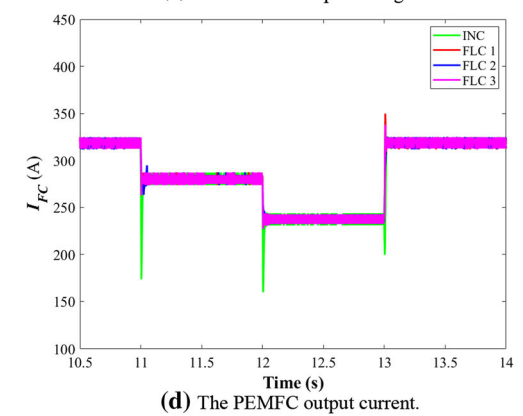
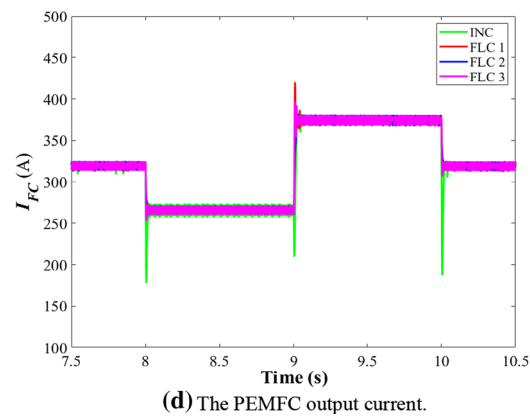
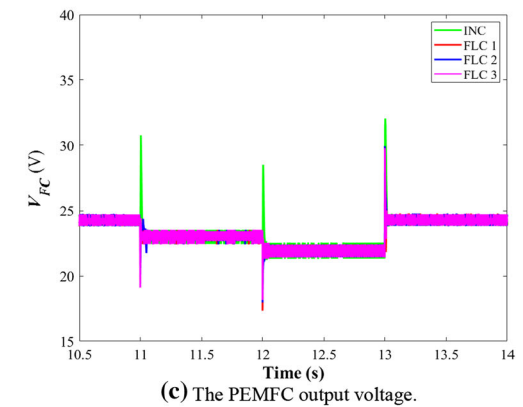
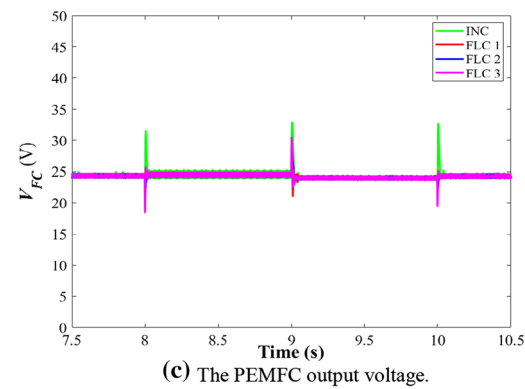
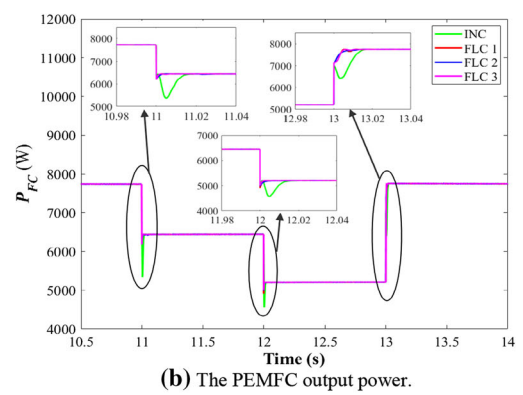
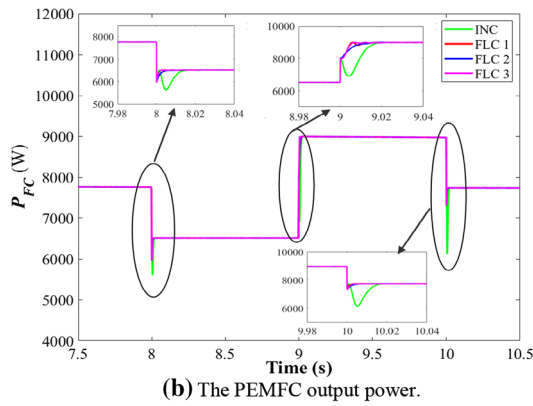
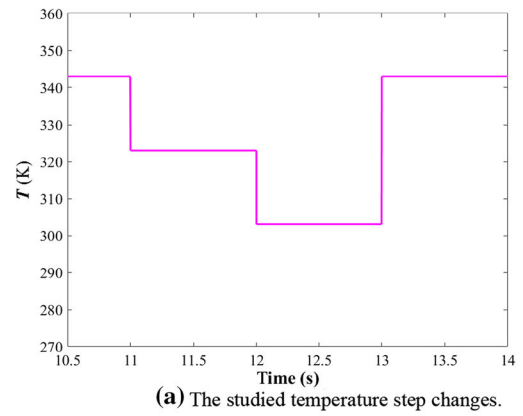
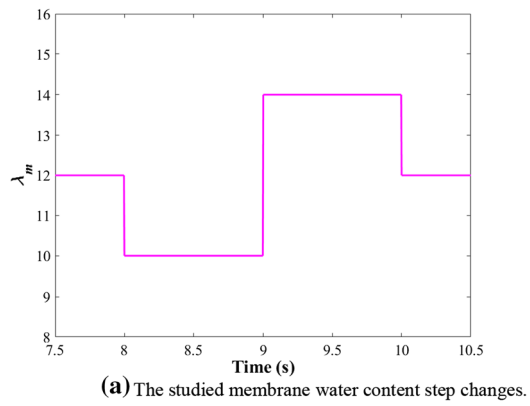


Fig. 8 Performance verification and comparison of the proposed FLC method at variations of membrane water content

Fig. 9 Performance verification and comparison of the proposed FLC method at variations of temperature

overshoot/undershoot in the output power is reduced in the proposed method, which enables the safe operation of the PEMFC.

Figure 9c compared the response of the PEMFC output voltage under the different MPPT methods. The proposed method enables the reduction of the PEMFC outputted voltage fluctuations at the different studied scenarios. In addition, the proposed method achieves minimized overshoots/undershoots under the studied temperature step changes. Figure 9d shows the output current waveforms under the various studied MPPT methods. It can be observed that the proposed MPPT method provides reduced overshoots/undershoots in the outputted current from the PEMFC. From another side, the traditional methods have high fluctuations and increase/decrease of the output current at various studied step changes. This would result in reduction of the operating lifetime of PEMFCs under the traditional methods compared to the proposed method.

In the aforementioned results, the performance of proposed MPPT method is compared to traditional methods during the starting transients, membrane water content variations, and temperature variations. In all cases, the proposed method achieves fast tracking of MPPT with reduced overshoot/undershoot values. This in turn advantageous in applications that require fast control of power stages. Additionally, reducing the overshoot/undershoot values result in improving the operating lifetime of PEMFC systems and power electronics converters as well. The results also show the reduced fluctuations of the output waveforms using the proposed method in steady state. This in turn confirms the smooth operation of the proposed method with reduced ripples. High ripple values have side-effects on the thermal, efficiency and lifetime performance of the various electrical components.

It can be seen that the main objective of the proposed MPPT method is to extract the maximum power from the PEMFC source while maintaining improved performance of the system. The main performance criteria for evaluating and comparing the robustness of MPPT controllers includes:

- The amount of the extracted power of the source.
- Capability of tracking the MPP at various operating membrane water content and temperature combination.
- The settling time to reach steady state.
- The oscillations and/or ripples of the output power, voltage, and current waveforms of PEMFCs at steady state.
- The overshoot/undershoot values at transient step changes in the system.

Based on the aforementioned results and analysis, the proposed method is advantageous as following:

- It uses only measured electrical waveforms (voltage and current) from the PEMFC source. It does not need complex sensors such as membrane water content and/or temperature sensors.
- It achieves variable and adaptive step size for MPPT control compared to fixed step size P and O and HC methods.
- It is based on FLC approach, which makes it feasible for simple and low cost digital control implementation.
- The proposed method is capable of extracting the maximum power from PEMFC at various operating conditions.
- It has reduced settling time for MPPT without oscillations.
- It achieves reduced oscillations and/or ripples of the output power, voltage, and current waveforms of PEMFCs at steady state.
- It has decreased values of overshoot/undershoot values at transient step changes in the system.

4 Conclusion

In this paper, the performance of PEMFC systems is improved through proposing FLC MPPT method. The proposed method advantages are the lower number of employed sensors, fast MPPT extraction, lower overshoot/undershoot performance, and smooth steady state performance. The mathematical model of the PEMFC is implemented with the power and control circuits in Matlab. The proposed MPPT method is compared to the widely used INC MPPT method and the various proposed FLC designs. The results show the improved performance of PEMFC system under the proposed FLC MPPT method compared to the INC method. The settling time has been reduced to 50% in the proposed FLC MPPT compared to the INC MPPT method. In addition, the overshoots in output current in addition to the undershoots in the output voltage are totally eliminated in the proposed MPPT method compared to the INC MPPT method. The proposed design method is advantageous at prolonging the operating lifetime of PEMFCs due to the reduction of overshoots/undershoots values. The proposed method is general and can be applied for enhancing the energy efficiency extraction in various PEMFC applications, including electric vehicles (EVs), renewable energy systems, unmanned aerial vehicle (UAV), etc.

Author contributions All authors collaborated and contributed equally to this work. All authors have read and agreed to the published version of the manuscript.

Funding This work was supported by the Chilean Government through Projects SERC Chile (ANID/FONDAP15110019), and AC3E (ANID/Basal/FB0008).

Declarations

Conflict of interest The authors declare no conflict of interest.

References

- Ali A, Raisz D, Mahmoud K (2019) Optimal oversizing of utility-owned renewable DG inverter for voltage rise prevention in MV distribution systems. *Int J Electr Power Energy Syst* 105:500–513. <https://doi.org/10.1016/j.ijepes.2018.08.040>
- Mahmoud K, Abdel-Nasser M (2019) Fast yet accurate energy-loss-assessment approach for analyzing/sizing PV in distribution systems using machine learning. *IEEE Trans Sustain Energy* 10(3):1025–1033. <https://doi.org/10.1109/TSTE.2018.2859036>
- Aly M, Ramadan HA (2019) Design and implementation of adaptive SVPWM algorithm for multilevel inverters in renewable energy applications. *Sol Energy* 183:745–754. <https://doi.org/10.1016/j.solener.2019.03.069>
- Aly M, Ahmed EM, Shoyama M (2017) Thermal and reliability assessment for wind energy systems with DSTATCOM functionality in resilient microgrids. *IEEE Trans Sustain Energy* 8(3):953–965. <https://doi.org/10.1109/TSTE.2016.2635200>
- Said SM, Aly M, Hartmann B, Alharbi AG, Ahmed EM (2019) SMES-based fuzzy logic approach for enhancing the reliability of microgrids equipped with PV generators. *IEEE Access* 7:92059–92069. <https://doi.org/10.1109/ACCESS.2019.2927902>
- Alhaider MM, Ahmed EM, Aly M, Serhan HA, Mohamed EA, Ali ZM (2020) New temperature-compensated multi-step constant-current charging method for reliable operation of battery energy storage systems. *IEEE Access* 8:27961–27972. <https://doi.org/10.1109/ACCESS.2020.2972391>
- Habib M, Ladjici AA, Harrag A (2020) Microgrid management using hybrid inverter fuzzy-based control. *Neural Comput Appl* 32(13):9093–9111. <https://doi.org/10.1007/s00521-019-04420-5>
- Puranik I, Zhang L, Qin J (2018) Impact of low-frequency ripple on lifetime of battery in MMC-based battery storage systems. In: 2018 IEEE energy conversion congress and exposition (ECCE), Portland, OR, pp 2748–2752. <https://doi.org/10.1109/ECCE.2018.8558061>
- Eid A (2014) Utility integration of PV-wind-fuel cell hybrid distributed generation systems under variable load demands. *Int J Electr Power Energy Syst* 62:689–699. <https://doi.org/10.1016/j.ijepes.2014.05.020>
- Tang Y, Bu C, Liu M, Zhang L, Lian Q (2018) Application of ELM–Hammerstein model to the identification of solid oxide fuel cells. *Neural Comput Appl* 29(2):401–411. <https://doi.org/10.1007/s00521-016-2453-y>
- El-Hay EA, El-Hameed MA, El-Fergany AA (2019) Improved performance of PEM fuel cells stack feeding switched reluctance motor using multi-objective dragonfly optimizer. *Neural Comput Appl* 31(11):6909–6924. <https://doi.org/10.1007/s00521-018-3524-z>
- Wang Y, Wang Y, Chen G (2020) Robust composite adaptive neural network control for air management system of PEM fuel cell based on high-gain observer. *Neural Comput Appl* 32(14):10229–10243. <https://doi.org/10.1007/s00521-019-04561-7>
- Lü X, Qu Y, Wang Y, Qin C, Liu G (2018) A comprehensive review on hybrid power system for PEMFC-HEV: issues and strategies. *Energy Convers Manag* 171:1273–1291. <https://doi.org/10.1016/j.enconman.2018.06.065>
- Liu G et al (2020) Thermodynamic modeling and analysis of a novel PEMFC-ORC combined power system. *Energy Convers Manag* 217:112998. <https://doi.org/10.1016/j.enconman.2020.112998>
- Chitsaz A, Haghghi MA, Hosseinpour J (2019) Thermodynamic and exergoeconomic analyses of a proton exchange membrane fuel cell (PEMFC) system and the feasibility evaluation of integrating with a proton exchange membrane electrolyzer (PEME). *Energy Convers Manag* 186:487–499. <https://doi.org/10.1016/j.enconman.2019.03.004>
- Chen X et al (2021) Thermodynamic and economic study of PEMFC stack considering degradation characteristic. *Energy Convers Manag* 235:114016. <https://doi.org/10.1016/j.enconman.2021.114016>
- Yin L, Li Q, Chen W, Wang T, Liu H (2019) Experimental analysis of optimal performance for a 5 kW PEMFC system. *Int J Hydrog Energy* 44(11):5499–5506. <https://doi.org/10.1016/j.ijhydene.2018.08.157>
- Lee JY, Lee JH, Kim TS (2019) Thermo-economic analysis of using an organic Rankine cycle for heat recovery from both the cell stack and reformer in a PEMFC for power generation. *Int J Hydrog Energy* 44(7):3876–3890. <https://doi.org/10.1016/j.ijhydene.2018.12.071>
- Yan H et al (2020) Techno-economic evaluation and technology roadmap of the MWe-scale SOFC-PEMFC hybrid fuel cell system for clean power generation. *J Clean Prod* 255:120225. <https://doi.org/10.1016/j.jclepro.2020.120225>
- Authayanun S, Hacker V (2018) Energy and exergy analyses of a stand-alone HT-PEMFC based trigeneration system for residential applications. *Energy Convers Manag* 160:230–242. <https://doi.org/10.1016/j.enconman.2018.01.022>
- Yang F, Huang N, Sun Q, Cheng L, Wennersten R (2018) Modeling and techno-economic analysis of the heat pump-integrated PEMFC-based micro-CHP system. *Energy Procedia* 152:83–88. <https://doi.org/10.1016/j.egypro.2018.09.063>
- Bayrak ZU, Kaya U, Oksuztepe E (2020) Investigation of PEMFC performance for cruising hybrid powered fixed-wing electric UAV in different temperatures. *Int J Hydrog Energy* 45(11):7036–7045. <https://doi.org/10.1016/j.ijhydene.2019.12.214>
- González-Espasandín Ó, Leo TJ, Raso MA, Navarro E (2019) Direct methanol fuel cell (DMFC) and H₂ proton exchange membrane fuel (PEMFC/H₂) cell performance under atmospheric flight conditions of Unmanned Aerial Vehicles. *Renew Energy* 130:762–773. <https://doi.org/10.1016/j.renene.2018.06.105>
- Jin J, Hu M, Zhao X (2020) Investigation of incorporating oxygen into TiN coating to resist high potential effects on PEMFC bipolar plates in vehicle applications. *Int J Hydrog Energy* 45(43):23310–23326. <https://doi.org/10.1016/j.ijhydene.2020.06.059>
- Wu Z et al (2019) Dynamic modeling and operation strategy of an NG-fueled SOFC-WGS-TSA-PEMFC hybrid energy conversion system for fuel cell vehicle by using MATLAB/SIMULINK. *Energy* 175:567–579. <https://doi.org/10.1016/j.energy.2019.03.119>
- Arévalo P, Cano A, Jurado F (2020) Comparative study of two new energy control systems based on PEMFC for a hybrid tramway in Ecuador. *Int J Hydrog Energy* 45(46):25357–25377. <https://doi.org/10.1016/j.ijhydene.2020.06.212>
- Peng F et al (2017) Development of master-slave energy management strategy based on fuzzy logic hysteresis state machine and differential power processing compensation for a PEMFC-LIB-SC hybrid tramway. *Appl Energy* 206:346–363. <https://doi.org/10.1016/j.apenergy.2017.08.128>

28. Aly M, Rezk H (2020) A differential evolution-based optimized fuzzy logic MPPT method for enhancing the maximum power extraction of proton exchange membrane fuel cells. *IEEE Access* 8:172219–172232. <https://doi.org/10.1109/ACCESS.2020.3025222>
29. Benyahia N et al (2014) MPPT controller for an interleaved boost dc–dc converter used in fuel cell electric vehicles. *Int J Hydrog Energy* 39(27):15196–15205. <https://doi.org/10.1016/j.ijhydene.2014.03.185>
30. Harrag A, Messalti S (2017) Variable step size IC MPPT controller for PEMFC power system improving static and dynamic performances. *Fuel Cells* 17(6):816–824. <https://doi.org/10.1002/fuce.201700047>
31. Rezk H, Fathy A (2020) Performance improvement of PEM fuel cell using variable step-size incremental resistance MPPT technique. *Sustainability* 12(14):5601. <https://doi.org/10.3390/su12145601>
32. Rana KPS, Kumar V, Sehgal N, George S (2019) A Novel dP/dI feedback based control scheme using GWO tuned PID controller for efficient MPPT of PEM fuel cell. *ISA Trans* 93:312–324. <https://doi.org/10.1016/j.isatra.2019.02.038>
33. Kler D, Rana KPS, Kumar V (2018) A nonlinear PID controller based novel maximum power point tracker for PV systems. *J Frankl Inst* 355(16):7827–7864. <https://doi.org/10.1016/j.jfranklin.2018.06.003>
34. Bahri H, Harrag A (2021) Ingenious golden section search MPPT algorithm for PEM fuel cell power system. *Neural Comput Appl*. <https://doi.org/10.1007/s00521-020-05581-4>
35. Cao Y, Li Y, Zhang G, Jermstittiparsert K, Nasser M (2020) An efficient terminal voltage control for PEMFC based on an improved version of whale optimization algorithm. *Energy Rep* 6:530–542. <https://doi.org/10.1016/j.egyr.2020.02.035>
36. Nanadegani FS, Lay EN, Iranzo A, Salva JA, Sunden B (2020) On neural network modeling to maximize the power output of PEMFCs. *Electrochim Acta* 348:136345. <https://doi.org/10.1016/j.electacta.2020.136345>
37. Reddy KJ, Sudhakar N (2019) ANFIS-MPPT control algorithm for a PEMFC system used in electric vehicle applications. *Int J Hydrog Energy* 44(29):15355–15369. <https://doi.org/10.1016/j.ijhydene.2019.04.054>
38. Jyotheeswara Reddy K, Sudhakar N (2018) A new RBFN based MPPT controller for grid-connected PEMFC system with high step-up three-phase IBC. *Int J Hydrog Energy* 43(37):17835–17848. <https://doi.org/10.1016/j.ijhydene.2018.07.177>
39. Ahmadi S, Abdi Sh, Kakavand M (2017) Maximum power point tracking of a proton exchange membrane fuel cell system using PSO-PID controller. *Int J Hydrog Energy* 42(32):20430–20443. <https://doi.org/10.1016/j.ijhydene.2017.06.208>
40. Harrag A, Bahri H (2017) Novel neural network IC-based variable step size fuel cell MPPT controller. *Int J Hydrog Energy* 42(5):3549–3563. <https://doi.org/10.1016/j.ijhydene.2016.12.079>
41. Jyotheeswara Reddy K, Sudhakar N (2018) High voltage gain interleaved boost converter with neural network based MPPT controller for fuel cell based electric vehicle applications. *IEEE Access* 6:3899–3908. <https://doi.org/10.1109/ACCESS.2017.2785832>
42. Rezk H, Aly M, Al-Dhaifallah M, Shoyama M (2019) Design and hardware implementation of new adaptive fuzzy logic-based MPPT control method for photovoltaic applications. *IEEE Access* 7:106427–106438. <https://doi.org/10.1109/ACCESS.2019.2932694>
43. Al Nabulsi A, Dhaouadi R (2012) Efficiency optimization of a DSP-based standalone PV system using fuzzy logic and dual-MPPT control. *IEEE Trans Ind Inform* 8(3):573–584. <https://doi.org/10.1109/TII.2012.2192282>
44. Mule S, Hardas R, Kulkarni NR (2016) P&O, IncCon and fuzzy logic implemented MPPT scheme for PV systems using PIC18F452. In: 2016 International conference on wireless communications, signal processing and networking (WiSPNET), Chennai, India, pp 1320–1325. <https://doi.org/10.1109/WiSPNET.2016.7566351>
45. Aly M, Rezk H (2021) A MPPT based on optimized FLC using manta ray foraging optimization algorithm for thermo-electric generation systems. *Int J Energy Res*. <https://doi.org/10.1002/er.6728>
46. Khan MJ, Mathew L (2019) Fuzzy logic controller-based MPPT for hybrid photo-voltaic/wind/fuel cell power system. *Neural Comput Appl* 31(10):6331–6344. <https://doi.org/10.1007/s00521-018-3456-7>
47. Said SM, Aly M, Balint H (2020) An efficient reactive power dispatch method for hybrid photovoltaic and superconducting magnetic energy storage inverters in utility grids. *IEEE Access* 8:183708–183721. <https://doi.org/10.1109/access.2020.3029326>
48. Salama HS, Said SM, Aly M, Vokony I, Hartmann B (2021) Studying impacts of electric vehicle functionalities in wind energy-powered utility grids with energy storage device. *IEEE Access* 9:45754–45769. <https://doi.org/10.1109/ACCESS.2021.3066877>
49. Aly M, Ahmed EM, Rezk H, Mohamed EA (2021) Marine predators algorithm optimized reduced sensor fuzzy-logic based maximum power point tracking of fuel cell-battery standalone applications. *IEEE Access* 9:27987–28000. <https://doi.org/10.1109/ACCESS.2021.3058610>
50. Harrag A, Rezk H (2021) Indirect P&O type-2 fuzzy-based adaptive step MPPT for proton exchange membrane fuel cell. *Neural Comput Appl*. <https://doi.org/10.1007/s00521-021-05729-w>
51. Menesy AS, Sultan HM, Korashy A, Kamel S, Jurado F (2021) A modified farmland fertility optimizer for parameters estimation of fuel cell models. *Neural Comput Appl*. <https://doi.org/10.1007/s00521-021-05821-1>
52. Mossa MA, Kamel OM, Sultan HM, Diab AAZ (2020) Parameter estimation of PEMFC model based on Harris Hawks' optimization and atom search optimization algorithms. *Neural Comput Appl*. <https://doi.org/10.1007/s00521-020-05333-4>
53. Kumar YS, Gupta R (2012) Maximum power point tracking of multiple photovoltaic arrays. In: 2012 Students conference on engineering and systems, Allahabad, Uttar Pradesh, India, pp 1–6. <https://doi.org/10.1109/SCES.2012.6199027>
54. Hauke B (2015) Basic calculation of a boost converter's power stage. *Tex Instrum*. <https://doi.org/10.4000/nuevomundo.30565>
55. Al-Majidi SD, Abbod MF, Al-Rawashidy HS (2018) A novel maximum power point tracking technique based on fuzzy logic for photovoltaic systems. *Int J Hydrog Energy* 43(31):14158–14171. <https://doi.org/10.1016/j.ijhydene.2018.06.002>
56. Chen C-H, Jeng S-Y, Lin C-J (2020) Mobile robot wall-following control using fuzzy logic controller with improved differential search and reinforcement learning. *Mathematics* 8(8):1254. <https://doi.org/10.3390/math8081254>
57. Carnero MC (2020) Fuzzy multicriteria models for decision making in gamification. *Mathematics* 8(5):682. <https://doi.org/10.3390/math8050682>

Publisher's Note Springer Nature remains neutral with regard to jurisdictional claims in published maps and institutional affiliations.